

Attosecond Strobng of Two-Surface Population Dynamics in Dissociating H_2^+

A. Staudte,^{1,2,*} D. Pavičić,² S. Chelkowski,⁴ D. Zeidler,² M. Meckel,¹ H. Niikura,² M. Schöffler,¹ S. Schössler,¹ B. Ulrich,¹ P. P. Rajeev,² Th. Weber,¹ T. Jahnke,¹ D. M. Villeneuve,² A. D. Bandrauk,⁴ C. L. Cocke,³ P. B. Corkum,² and R. Dörner¹

¹*Institut für Kernphysik, J. W. Goethe Universität, D-60486 Frankfurt/Main, Germany*

²*National Research Council, 100 Sussex Drive, Ottawa, Ontario, Canada K1A 0R6*

³*J. R. Macdonald Laboratory, Kansas State University, Manhattan, Kansas 66506, USA*

⁴*Laboratoire de Chimie Théorique, Faculté des Sciences, Université de Sherbrooke, Sherbrooke, Québec, Canada J1K 2R1*

(Received 7 June 2006; published 14 February 2007)

Using H_2^+ and D_2^+ , we observe two-surface population dynamics by measuring the kinetic energy of the correlated ions that are created when H_2^+ (D_2^+) ionize in short (40–140 fs) and intense (10^{14} W/cm²) infrared laser pulses. Experimentally, we find a modulation of the kinetic energy spectrum of the correlated fragments. The spectral progression arises from a hitherto unexpected spatial modulation on the excited state population, revealed by Coulomb explosion. By solving the two-level time-dependent Schrödinger equation, we show that an interference between the net-two-photon and the one-photon transition creates localized electrons which subsequently ionize.

DOI: 10.1103/PhysRevLett.98.073003

PACS numbers: 33.80.Rv, 33.80.Gj, 42.50.Hz

The interplay of population between two isolated electronic levels is the major tool in quantum optics and molecular science. In molecular science, controlling electronic excitation controls the bond. This is used to make cold molecules from cold atoms (e.g., [1]). It is also used to break symmetry in molecules [2,3]. Even nonresonant population transfer can control reaction pathways [4].

We report the observation of electronic population dynamics—as it occurs. As illustrated in Fig. 1, we use the ground ($1s\sigma_g$) and first excited states ($2p\sigma_u$) of H_2^+ as our two-level system. The $1s\sigma_g$ and $2p\sigma_u$ states are isolated from all other electronic levels, dipole coupled, and degenerate in the separated atom limit. Experimentally, we prepare the H_2^+ by ionizing H_2 in an intense infrared laser pulse. Components of the vibrational wave packet created by tunnel ionization can sweep through both the one- and three-photon resonances between the two surfaces. Population is transferred from $1s\sigma_g$ to $2p\sigma_u$ via adiabatic rapid passage (the general term given to these processes in quantum optics) or bond softening (the term used in strong field molecular physics) [5,6]. In our experiment, which uses near infrared light, a snapshot of the upper state population is taken within a time window of a few hundred attoseconds via Coulomb explosion imaging. This snapshot is repeated every half laser cycle, i.e., each 1.3 fs (800 nm) to 2.3 fs ($1.4 \mu\text{m}$).

We find a sequence of spectroscopic lines in the kinetic energy spectrum of the protons or deuterons formed during enhanced ionization (EI) of H_2 and D_2 [7–9]. The lines appear for both linear and circular polarizations and at all wavelengths (800 nm– $1.4 \mu\text{m}$) and pulse durations (40–140 fs) that we have studied. We obtain quantitative agreement between theory and experiment using a two-surface model for H_2^+ sampled by ionization at the peak of the field with an ionization rate taken from preceding work.

Thus, we establish the origins of the modulation in the two-level dynamics of dissociating H_2^+ (D_2^+). It reflects a previously unrecognized spatial structure of the electronic excitation in the molecular ion.

Our work relates to early observations of EI. Then, weak modulations in the proton energy spectrum were interpreted as light-induced bound states [10] and as signatures of an increased ionization probability at discrete internuclear separations [11]. Recently, ion beam experiments have renewed the interest in spectral modulation in the enhanced ionization region as a measure of the vibrational structure [12] or channel opening in multiphoton ionization [13].

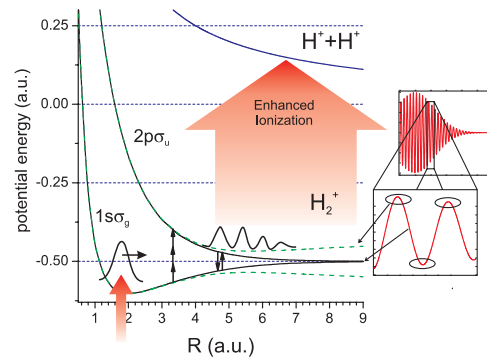


FIG. 1 (color online). Sketch of the time-dependent two-level system in H_2^+ . The two surfaces are shown for maximum (dashed line) and the zero crossing (solid line) of the laser field. Tunneling ionization of the neutral molecule creates a wave packet that rapidly moves towards the outer turning point. The two dissociation pathways, net-two-photon (absorption of 3 and reemission of 1 photon) and one-photon, interfere on the quasi-static upper state. Enhanced ionization samples the population on this surface at the field maximum of each half laser cycle.

The experiment was performed using cold target recoil ion momentum spectroscopy [14]. The cold target ($\ll 10$ K) is a gas jet that is created in a supersonic expansion of H_2 and D_2 precooled to 50 K. With a nozzle diameter of $11 \mu\text{m}$ and a stagnation pressure of >2 bar, the speed ratio is >20 .

Femtosecond laser pulses (40–140 fs) of different wavelengths (800 nm, $1.2 \mu\text{m}$, and $1.4 \mu\text{m}$) were focused to peak intensities of $1.0\text{--}4.5 \times 10^{14} \text{ W/cm}^2$ into the gas jet of unaligned H_2 and D_2 . The peak intensity was determined using the radial electron and ion momentum of single ionization in circularly polarized light [15]. The uncertainty in the peak intensity is $\approx 10\%$ at 800 nm and 30% at 1.2 and $1.4 \mu\text{m}$. We determined the pulse duration using a second-harmonic generation autocorrelator for all wavelengths with an uncertainty of $\pm 10\%$.

Ions and electrons created in the focus are guided by electric and magnetic fields (23 V/cm, 12 G) towards two channel plate detectors with delay line position encoding. Ion momenta of up to 30 a.u. are collected with a 4π solid angle. Although we measured electrons and ions in coincidence, we will show only ion spectra here. However, correlated ion and electron momenta determine an overall spectrometer momentum resolution of ± 0.1 a.u. along and ± 0.5 a.u. perpendicular to the spectrometer axis.

Balancing peak intensity and target density, we ensured that the overall ion count rate was between 10^{-4} and 1 ion per laser shot. Therefore, space charge effects can be excluded. The kinetic energy release (KER) is computed in the molecular center-of-mass (c.m.) frame. We exclude random coincidences efficiently by restricting the c.m.

momentum to less than 3 a.u. Further details on the experimental setup can be found in Ref. [16].

Figure 2(a) shows the kinetic energy release of correlated proton and deuteron pairs in linearly polarized light. Both isotopes were simultaneously measured by means of a $\approx 1:1$ gas mixture. Hence, the difference in ionization yield arises from the different time scales of dissociation for isotopes. Furthermore, the isotope influences the position of the spectral lines.

Recollision can play a major role in dissociation dynamics of molecular hydrogen (see, e.g., [2,17,18]). However, in circularly polarized light, recollision is suppressed. Figure 2(b) shows that recollision does not contribute to the structure in the energy spectrum. Since it is the electric field of the laser that governs the molecular response, the intensity was doubled for circular polarization.

Figure 2(c) examines the intensity dependence of the spectral lines. Whereas increasing intensity blurs the feature, it does not affect the line position.

In Fig. 2(d), we changed the pulse duration while keeping the peak intensity constant. The line intensity is shifted from the high energy lines to the lower energetic lines when the pulse duration is increased. Again, the peak positions remain unaffected.

Figure 3 presents the KER spectra of D_2 obtained using 800 nm, $1.2 \mu\text{m}$, and $1.4 \mu\text{m}$ light. All three cases behave similarly. Although the overall structures of the enhanced ionization curves change, there is always a spectral progression. However, the positions of the peaks shift to lower energy with increasing wavelength.

There are two contributions to the kinetic energy release. First, the H_2^+ gains kinetic energy from the multiphoton Raman transitions that guide the wave packet as it moves to the region where enhanced ionization takes place. We observe the final H^+ kinetic energy as bond softening

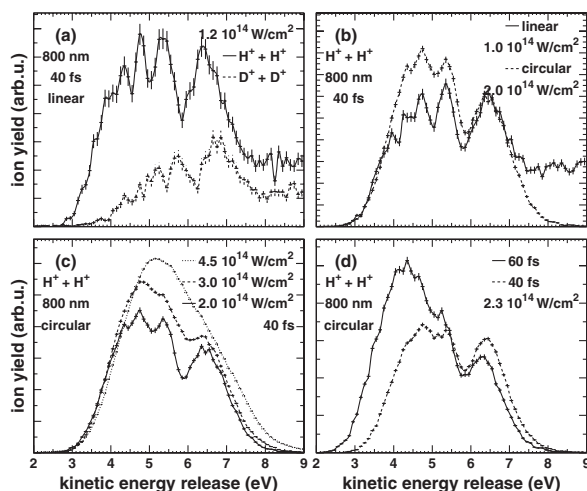


FIG. 2. KER spectra of proton and deuteron pairs from EI. Dependence of the spectral modulation on experimental parameters. The error bars are purely statistical (\sqrt{N} , N —ion yield). (a) Isotope [$N_{\text{max}} = 340, 158$ (top-bottom)], (b) polarization [$N_{\text{max}} = 660, 2.3 \times 10^3$ (top-bottom)], (c) peak intensity [$N_{\text{max}} = 5.3 \times 10^4, 1 \times 10^4, 2.3 \times 10^3$ (top-bottom)], and (d) pulse duration [$N_{\text{max}} = 2.6 \times 10^3, 4.1 \times 10^3$ (top-bottom)].

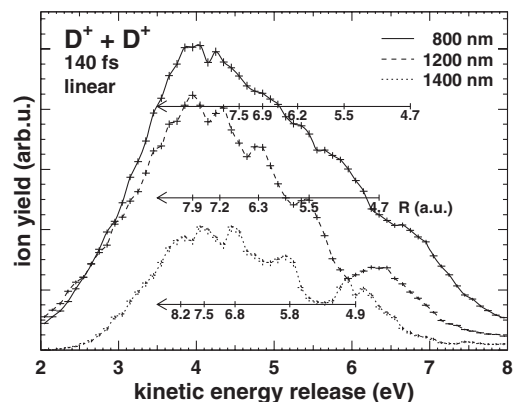


FIG. 3. Deuteron KER spectra for different wavelengths of laser radiation and similar pulse duration. The superimposed scales show R (a.u.) with $R = 1/(\text{KER} - \bar{E}_{\text{diss}})$. 800 nm: $2.5 \times 10^{14} \text{ W/cm}^2$, $\bar{E}_{\text{diss}} = 0.93 \text{ eV}$; 1200 nm: $1 \times 10^{14} \text{ W/cm}^2$, $\bar{E}_{\text{diss}} = 0.50 \text{ eV}$; 1400 nm: $0.6 \times 10^{14} \text{ W/cm}^2$, $\bar{E}_{\text{diss}} = 0.48 \text{ eV}$. $N_{\text{max}} = 4.7 \times 10^3, 4.1 \times 10^3, 680$ (top-bottom).

ing peaks in the case of those molecules that escape enhanced ionization. In all of our experiments, the KER of the $H^+ + H$ channel is ≤ 1.25 eV. Second, Coulomb explosion adds to the kinetic energy. Since the spectral progression that we observe lies between 3–7 eV, Coulomb explosion dominates. Hence, the second ionization occurs at $R \sim 5$ –10 a.u. In Fig. 3, we have included a scale for each wavelength that maps the kinetic energy release to internuclear separation according to $R = 1/(\text{KER} - \bar{E}_{\text{diss}})$, where \bar{E}_{diss} is the average dissociation energy as measured in the $D^+ + D$ channel.

We have solved the three-body 1-dimensional time-dependent Schrödinger equation [19] and obtained very good agreement of the peak spacing with experiment (not shown). However, since such a complete simulation does not provide easy insight, we will present these results in a forthcoming publication.

We now show that the spectral modulation arises from the interplay between electronic population dynamics and a vibrational wave packet, which produces a spatially modulated population in the quasistatic upper state. The upper state population is sampled by field ionization twice per laser period with a 360 as (800 nm)–620 as (1400 nm) sampling window (FWHM). Coulomb explosion reveals the R -dependent structure.

We model the nuclear dynamics using the two-surface time-dependent Schrödinger equation in which the complete wave function $\psi(\vec{r}_{\text{el}}, R, t)$ is approximated as a superposition of two electronic eigenfunctions $\varphi_g^{\text{el}}(\vec{r}_{\text{el}}, R)$ and $\varphi_u^{\text{el}}(\vec{r}_{\text{el}}, R)$ (gerade and ungerade):

$$\psi(\vec{r}_{\text{el}}, R, t) = \psi_g(R, t)\varphi_g^{\text{el}}(\vec{r}_{\text{el}}, R) + \psi_u(R, t)\varphi_u^{\text{el}}(\vec{r}_{\text{el}}, R). \quad (1)$$

Inserting the above equation into the time-dependent Schrödinger equation describing the full electron-nuclear dynamics (we assume that the laser electric field is parallel to the molecular axis and limit the nuclear dynamics to 1D along the z axis) yields two coupled differential equations for the nuclear functions $\psi_g(R, t)$ and $\psi_u(R, t)$ described by Eq. (15) in Ref. [20]. We solve these equations numerically, assuming that initially $\psi_u(R, 0) = 0$ and $\psi_g(R, 0)$ is equal to the vibrational ground state $v = 0$ of H_2 (D_2). This is equivalent to assuming that, during the ionization of H_2 , the nuclei remained frozen and a direct vertical Franck-Condon-like transition from H_2 to H_2^+ takes place [20]. We use an artificial laser pulse envelope, which rises from zero to its maximal value with the first two laser cycles and then falls as Gaussian with the experimental parameters. We assume that the tunnel (or overbarrier) instantaneous ionization occurs at each half-cycle of the laser field when the electric field reaches maximum or minimum from the upper (adiabatic, field following [21]) eigenstate

$$\Psi_2(t_k) = [1 + a^2]^{-1/2}(\varphi_u^{\text{el}} - a\varphi_g^{\text{el}}), \quad (2)$$

$$a = \frac{RE(t)}{V_u - V_g + \sqrt{(V_u - V_g)^2 + R^2E(t)^2}}$$

of the molecular electronic Hamiltonian plus the laser interaction term $E(t_k)z_{\text{el}}$ [see Eqs. (1)–(4) in Ref. [21] for details], with $t_k = kT_{\text{las}}/2$, where $k = 1, 2, 3, \dots$. T_{las} is the laser period, and $V_g(R)$ and $V_u(R)$ are the zero-field Born-Oppenheimer (gerade and ungerade, respectively) potentials of H_2^+ . The ionization rates (at fixed R) from the lower eigenstate $\Psi_1(t_k)$ are typically 2–4 orders of magnitude smaller. In our model, we project the time-dependent state [Eq. (1)] on the adiabatic upper eigenstate $\Psi_2(t_k)$, which yields

$$\chi_2(R, t_k) = \langle \Psi_2(t_k) | \psi(\vec{r}_{\text{el}}, R, t_k) \rangle = (1 + a^2)^{-1/2}[\psi_u(R, t) - a\psi_g(R, t)]. \quad (3)$$

We calculate the Coulomb explosion spectrum $S(E_{\text{expl}})$ using the following relation:

$$S(E_{\text{expl}}) = \sum_{k=1}^{k_f} \left| \int_0^\infty \Psi_C(E_{\text{expl}}, R') \chi_2(R', t_k) dR' \right|^2 P_k(R), \quad (4)$$

where $P_k(R) = 1 - \exp\{-\Gamma[R, E(t_k)]\}$ are ionization probabilities calculated at $t - t_k$ and at $R = 1/E_{\text{expl}}$. The ionization rates Γ from the upper state $\Psi_2(R, t_k)$ were taken from Tables 1 and 2 in Ref. [22]. In Eq. (4), we perform the projection on the Coulomb wave $\Psi_C(E_{\text{expl}}, R)$ defined in Ref. [19]. The value of the index k_f is fixed by the requirement that the summation stops when the laser intensity $I(t)$ falls to $I_{\text{max}}/8$. Note that, at $R > 6$, Eq. (3) simplifies to

$$\chi_2(R, t) \simeq 2^{-1/2}[\psi_u(R, t) - \psi_g(R, t)E(t)/|E(t)|], \quad (5)$$

which describes the projection on the electron localized on

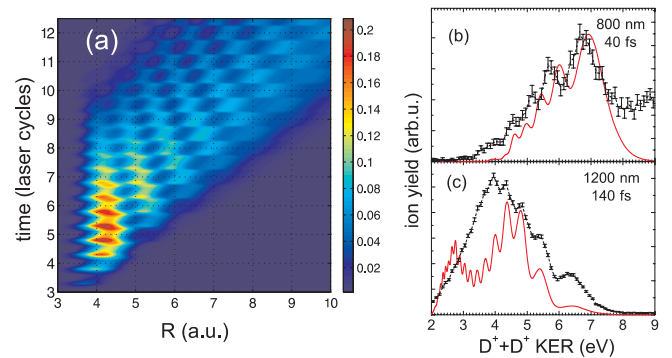


FIG. 4 (color online). (a) Simulated D_2^+ wave packet $|\chi_2(R, t)|^2$ at 800 nm, 1×10^{14} W/cm², and 40 fs. (b),(c) Comparison of simulated deuteron KER spectra with experiment at 800 and 1200 nm. Peak intensity: 1×10^{14} W/cm².

the left or right center. Also, asymptotically, $\psi_u(R, t)$ and $\psi_g(R, t)$ become proportional to $\exp(ik_u R)$ and $\exp(ik_g R)$, respectively, where k_u and k_g are the nuclear momenta corresponding to the one- or net-two-photon peak in the $H + p$ (or $D + D^+$) channels.

In Fig. 4, we compare the results of our model with the experimental data. Figure 4(a) shows the calculated population on the quasistatic upper surface plotted as a function of R and t . Sampling each $1/2$ laser period by field ionization and added incoherently, we obtain a very good agreement of the peak spacing with the experiment for different wavelengths [Figs. 4(b) and 4(c)]. Although not shown here, the simulation also reproduces the pulse duration, isotope, and intensity dependence of the experiment.

Hence, we have established the origin of the modulation on the two surfaces. From Eq. (5), we expect that effectively two plane waves will interfere, leading to the appearance of a cos-like structure in $|\chi_2(R)|^2$ and in the Franck-Condon factor present in Eq. (4). This interference leads to the minima in the probability shape $|\chi_2(R)|^2$ separated by $\pi/(k_g - k_u)$. The experimental value of $k_g - k_u$ is determined to be 3–3.4 a.u. This corresponds to a periodicity in $|\chi_2(R)|^2$ of $\Delta R \approx 1$ a.u., which is exactly what the simulation predicts [see Fig. 4(a)]. Thus, we arrive to the conclusion that the regular structures observed in the Coulomb explosion spectra originate from the interference of the net-two-photon with one-photon channels in Ψ_2 .

The intensity dependence is explained naturally: At higher intensity, the relative strength of the two dissociation channels becomes disparate. In fact, one would expect that the interference disappears at very low intensity when the net-two-photon channel is closed. However, at these intensities, double ionization is also strongly suppressed, obstructing a possible experimental detection.

In conclusion, we have observed an important new phenomenon—in the presence of an intense laser pulse, the electron population on the quasistatic upper potential energy surface of dissociating H_2^+ and D_2^+ has a strong R -dependent modulation. The total population is unmodulated because the lower level has the complementary population. It is the spatial equivalent of a two-level system where the population is transferred between the upper and lower states during Rabi oscillations, but the total population is fixed. We expect similar R -dependent population dynamics to occur in other dissociating molecules or during photoassociation of cold atoms during cold molecule formation.

We gratefully acknowledge inspiring discussions with O. Smirnova and M. Ivanov. The experimental work is supported by an NSERC accelerator grant, NSERC Centre-of-Excellence for Photonic Innovation, NRC HGF

science & technology fund, DFG, Alexander-von-Humboldt Stiftung, and the Studienstiftung des deutschen Volkes.

*Electronic address: andre.staudte@nrc.ca

- [1] B. Brown and I. Walmsley, *J. Phys. B* **39**, S1055 (2006).
- [2] M. Kling *et al.*, *Science* **312**, 246 (2006).
- [3] F. Martín, J. Fernáandez, T. Havermeier, L. Foucar, Th. Weber, K. Kreidi, M. Schöffler, L. Schmidt, T. Jahnke, O. Jagutzki, A. Czasch, E.P. Benis, T. Osipov, A.L. Landers, A. Belkacem, M.H. Prior, H. Schmidt-Böcking, C.L. Cocke, and R. Dörner, *Science* **315**, 629 (2007).
- [4] B. Sussman, D. Townsend, M. Ivanov, and A. Stolow, *Science* **314**, 278 (2006).
- [5] A. Giusti-Suzor, X. He, O. Atabek, and F. Mies, *Phys. Rev. Lett.* **64**, 515 (1990).
- [6] P. Bucksbaum, A. Zavriyev, H. Muller, and D. Schumacher, *Phys. Rev. Lett.* **64**, 1883 (1990).
- [7] J. Posthumus, L. Frasinski, A. Giles, and K. Codling, *J. Phys. B* **28**, L349 (1995).
- [8] K. Codling and L. Frasinski, *J. Phys. B* **26**, 783 (1993).
- [9] T. Zuo and A. Bandrauk, *Phys. Rev. A* **52**, R2511 (1995).
- [10] A. Zavriyev, P. Bucksbaum, J. Squier, and F. Salane, *Phys. Rev. Lett.* **70**, 1077 (1993).
- [11] G. Gibson, M. Li, C. Guo, and J. Neira, *Phys. Rev. Lett.* **79**, 2022 (1997).
- [12] D. Pavičić, A. Kiess, T. Hänsch, and H. Figger, *Phys. Rev. Lett.* **94**, 163002 (2005).
- [13] B. Esry, A. Saylor, P. Wang, K. Carnes, and I. Ben-Itzhak, *Phys. Rev. Lett.* **97**, 013003 (2006).
- [14] J. Ullrich, R. Moshhammer, A. Dorn, R. Dörner, L. Schmidt, and H. Schmidt-Böcking, *Rep. Prog. Phys.* **66**, 1463 (2003).
- [15] A. Alnaser, X. Tong, T. Osipov, S. Voss, C. Maharjan, B. Shan, Z. Chang, and C. Cocke, *Phys. Rev. A* **70**, 023413 (2004).
- [16] A. Staudte, Ph.D. thesis, J.W. Goethe Universität, Frankfurt/Main, 2005, www.atom.uni-frankfurt.de.
- [17] A. Alnaser, T. Osipov, E. Benis, A. Wech, B. Shan, C. Cocke, X. Tong, and C. Lin, *Phys. Rev. Lett.* **91**, 163002 (2003).
- [18] H. Niikura, F. Légaré, R. Hasbani, A. Bandrauk, M. Ivanov, D. Villeneuve, and P. Corkum, *Nature (London)* **417**, 917 (2002).
- [19] S. Chelkowski and A. Bandrauk, *Phys. Rev. A* **65**, 023403 (2002).
- [20] S. Chelkowski, M. Zamojski, and A. Bandrauk, *Phys. Rev. A* **63**, 023409 (2001).
- [21] H. Kono, Y. Sato, Y. Fujimura, and I. Kawata, *Laser Phys.* **13**, 883 (2003).
- [22] M. Plummer and J. McCann, *J. Phys. B* **29**, 4625 (1996).